Photoelectron diffraction from core levels and plasmon-loss peaks of aluminum

J. Osterwalder, T. Greber, S. Hüfner,* and L. Schlapbach
Institut de Physique, Université de Fribourg, CH-1700 Fribourg, Switzerland
(Received 8 January 1990)

Photoelectron diffraction has been measured from a (001) single-crystal surface of aluminum. Anisotropies of the photocurrent of 73% and 65% have been observed in azimuthal scans of 2*s* and 1*s* core-level intensities comprising the [011] direction. Azimuthal intensity scans have also been measured for the plasmon-loss peaks accompanying the 2*s* core lines. The forward-scattering-related intensity maxima along ⟨011⟩ directions are reduced with increasing plasmon number *n*. This suggests that defocusing effects due to multiple photoelectron scattering along rows of atoms are important. The rate at which the forward-scattering maxima are suppressed with increasing *n* indicates a defocusing length of the order of 45 Å in Al, which is longer than what had been previously calculated for the case of Cu. Furthermore, the invariance with *n* of diffraction features away from the [011] direction gives support to the idea that photoelectrons and Kikuchi electrons exhibit essentially the same diffraction effects.

INTRODUCTION

X-ray photoelectron diffraction (XPD) is a particular mode of detecting photoelectrons in a photoemission experiment that allows one to obtain structural information.[1,2] In short, the experiment consists of measuring the photoelectron current with high angular resolution from an oriented single crystal either under varying polar and azimuthal angles, or under fixed geometry as a function of the photon energy. The observed intensity variations of the photoelectron current can be analyzed in terms of the structure of the sample. Since photoelectrons have a relatively small mean free path, this technique can be used to study the surface atomic structure, which makes it a useful tool in modern surface science.

In order to be applicable as a general tool, the benefits and shortcomings of this technique should be known as thoroughly as possible. This is most easily achieved by studying XPD from single crystals of which the crystal structure is well known. So far mostly transition metals have been investigated, for the obvious reason that for them, good single crystals are available and also because they are frequently used as substrates for adsorbate studies. Hardly any XPD work has been done on the classical simple metals like Na, Mg, or Al. They have the advantage of a relatively simple, well-understood electronic structure[3,4] and a small atomic number *Z*, which should make an analysis of the data less complicated. In addition, they show well-developed plasmon losses, with a plasmon-creation mean free path Λ_{pl}, which is, approximately $1\frac{1}{2}$ times the total mean free path Λ_{tot}.[5–7]

Measuring XPD patterns of plasmon-loss peaks accompanying core lines allows us to vary the relative weight of the emitters contributing to the total intensity from different depths below the surface. We shall demonstrate how the effects of multiple-scattering processes, such as occurring along rows of atoms, can be investigated in this way. In this context it should be mentioned that the individual electron-atom scattering events that give rise to the observed diffraction patterns are strongly peaked into the forward direction at energies higher than a few hundred eV.[1] This can, in principle, be regarded as a focusing of the electron wave into directions of near-neighbor atoms. It has been suggested on the basis of multiple-scattering calculations,[8,9] that if more than one scattering atom is placed along the emission direction, these forward-scattering effects are markedly reduced due to a dephasing of the electron wave after passing the atoms nearest to the emitter. Already four atoms following an emitter can completely destroy the forward-scattering enhancement expected in a single-scattering theory. This effect has been termed defocusing.[8,9] It is the intention of this paper to gain some experimental insight into the importance of these defocusing effects. We shall also use our plasmon-loss XPD data to draw some qualitative conclusions about the scattering and diffraction of a related kind of inelastically scattered electrons, namely Kikuchi electrons.

We shall present XPD data from a (001) surface of Al, measured as a function of the azimuthal angle ϕ at a constant polar angle of $\theta=45°$ with respect to the surface normal. An extremely high anisotropy $A=(I_{max}-I_{min})/I_{max}$ of 73% is observed for the 2*s* line of Al ($E_{kin}=1136$ eV), if an angular resolution $\Delta\Omega$ of less than 1° is used, which just barely permits data taking with sufficient statistics in a reasonable time. For the 1*s* line, data with slightly less angular resolution of $\Delta\Omega \leq 3°$ yield $A=65\%$. These values are at least as large as those obtained for the classical test cases of Ni and Cu. The anisotropies measured in the plasmon lines decrease with increasing plasmon number.

EXPERIMENTAL

The experiments were performed with a modified VG ESCALAB Mark II spectrometer, equipped with a

three-detector unit that made the data accumulation with high angular resolution down to full acceptance cones of $\Delta\Omega < 1°$ possible. The spectrometer was equipped with a Mg $K\alpha$ ($\hbar\omega = 1253.6$ eV) and Si $K\alpha$($\hbar\omega = 1740.0$ eV) twin anode. The latter source allowed, with reasonable signal-to-background ratio, the measurement of the Al 1s line, with a binding energy E_B of 1560 eV. The angle between the **k** vectors of the x rays and the detected electrons is 54°. The crystal could be cleaned by argon-ion bombardment and heating to 600 K. After repeated cycles of bombardment and heating there were still small signals of C 1s and O 1s visible, corresponding to less than 10% of a monolayer, but no trace of oxidized Al could be detected in the Al core lines. Sharp low-energy electron diffraction (LEED) spots provided the picture of a well-ordered unreconstructed surface. The first surface plasmon could always be observed, which confirms the high quality of the sample. In the XPD measuring procedure the background under the photoemission lines was always immediately subtracted using a linear approximation, unless stated otherwise. The data presented in this paper were taken under a fixed polar angle of $\theta = 45°$, with respect to the surface normal, scanning the azimuthal angle ϕ. This results in a symmetry of the XPD patterns, which reflects the fourfold symmetry of the (001) surface.

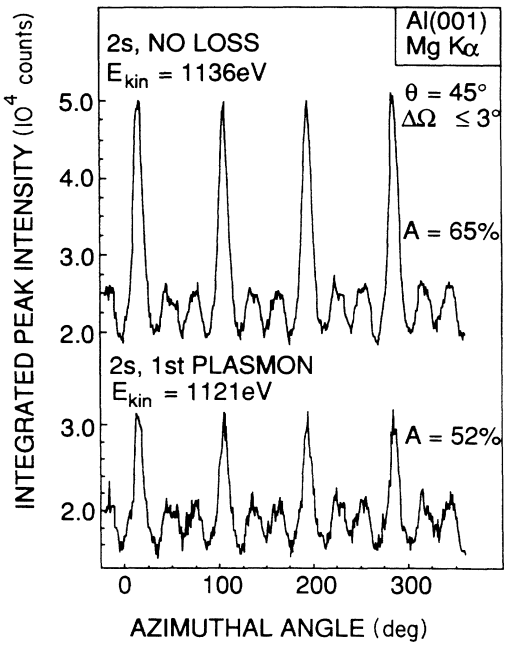

FIG. 1. Azimuthal XPD curves from a (001) single crystal of Al, measured with Mg $K\alpha$ radiation for the 2s core line ($E_B = 118$ eV) and the first associated plasmon-loss peak ($\hbar\omega_p = 15$ eV). The fixed polar angle was $\theta = 45°$, which results in a scanning through the ⟨011⟩ directions in 90° intervals, showing strong forward-scattering maxima. The intensity was determined during the measuring process by subtracting a linear background in an appropriate window around the peak. The total electron acceptance angle was $\Delta\Omega \leq 3°$. Note that the azimuthal angle scale shows an arbitrary offset corresponding to experimental manipulator settings.

RESULTS AND DISCUSSION

Data

A full 360° azimuthal scan at $\theta = 45°$ for the Al 2s line from Al(001) is shown in the top part of Fig. 1. The data clearly show the expected fourfold symmetry. The angles of the main peaks correspond to an electron detection along the ⟨011⟩ directions. The anisotropy is $A = 65\%$. These data were taken with an angular resolution of $\Delta\Omega \leq 3°$. The bottom part of Fig. 1 shows a corresponding scan with the energy window set on the first bulk-plasmon-loss peak accompanying the 2s line ($\hbar\omega_p = 15$ eV). The anisotropy still amounts to $A = 52\%$. In Fig. 2 similar data are given for energy windows set on the 2s core line and on the first, second, and, third plasmon-loss peak accompanying this line. Due to low count rates in the latter peaks, only slightly more than one quadrant of the fourfold geometry has been measured. The poorer statistics of the data of consecutive plasmon losses are a consequence of the decreasing signal-to-noise ratio in going from the 2s line to the plasmon-loss peaks (see Fig. 3).

Figure 3 shows energy spectra for the 2s and 1s lines in the ϕ position of maximum count rate along [011] and at $\Delta\phi = 45°$ off this direction. The energy spectra for both core lines show that the relative intensities of successive plasmon-loss peaks decrease slower for the off-symmetry

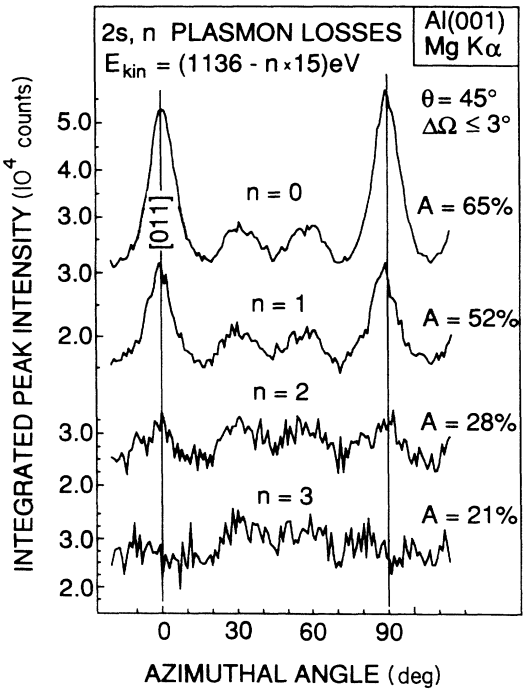

FIG. 2. Azimuthal XPD curves from a (001) single crystal of Al, measured with Mg $K\alpha$ radiation, for the 2s core level ($E_B = 118$ eV) and the first three ($n = 1,2$, and 3) associated plasmon-loss peaks ($\hbar\omega_p = 15$ eV). The polar angle was $\theta = 45°$. The scans in the azimuthal direction covered a range of 120°, including two ⟨011⟩ directions (main maxima for the no-loss line).

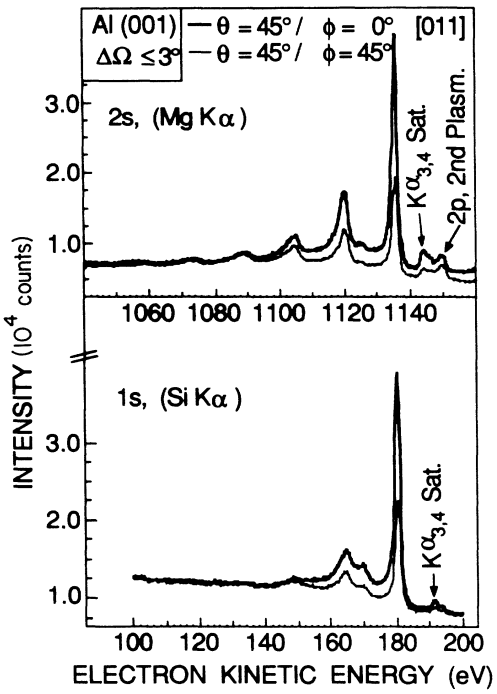

FIG. 3. Energy spectra from a (001) single crystal of Al. Top panel: Al 2*s* spectra, measured with Mg $K\alpha$ radiation ($\hbar\omega = 1253.6$ eV) at $\theta = 45°$ and $\phi = 0°$ along the [011] direction (bold line), i.e., in the intensity maxima in Fig. 1, and in a minimum of the diffraction intensity at $\phi = 45°$ away from [011] (thin line). Bottom panel: same as above, but for the Al 1*s* line measured with Si $K\alpha$ radiation ($\hbar\omega = 1740.0$ eV).

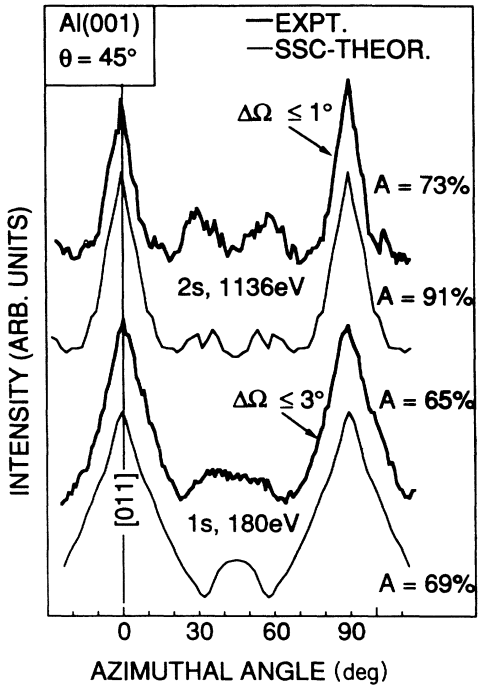

FIG. 4. Top two curves: Comparison of experimental (bold line) and theoretical (thin line) Al 2*s* XPD patterns from Al(001). The experimental electron acceptance angle was set to $\Delta\Omega \leq 1°$ and Mg $K\alpha$ radiation was used for excitation. The theoretical curve represents a single-scattering calculation with a $3\times3\times3$ unit-cell cluster. Bottom two curves: same as above for the Al 1*s* core line, but Si $K\alpha$ radiation has been used for excitation, and the acceptance angle was set to $\Delta\Omega \leq 3°$.

direction than for the [011] direction, in agreement with the data in Fig. 2.

In Fig. 4 azimuthal scans for the 2*s* and 1*s* lines are compared for an angular range of 120°. For these two lines the kinetic energy is very different, namely, 1136 eV (2*s*, Mg $K\alpha$) and 180 eV (1*s*, Si $K\alpha$), which corresponds to electron mean free paths of ≈ 20 and ≈ 5 Å, respectively.[6] The data for the 2*s* line have been taken with a resolution of $\Delta\Omega \leq 1°$ in order to check whether there are any structures in the curves, which are lost by using a resolution of $\Delta\Omega \leq 3°$. This does not seem to be the case.

While, at present it is not possible to give a comprehensive theoretical analysis of the data in Figs. 1–3, they can be used to arrive at some qualitative conclusions. In the following discussion, the fact that the spectra contain not only the extrinsic but also an intrinsic contribution will be neglected. The term extrinisic here stands for that part of the spectrum that is produced in the "normal" photoemission process: photoexcitation, travel to the surface and creation of bulk losses, and escape through the surface creating surface losses; in contrast, the intrinsic part consists of the electron-hole pairs accompanying the main line and those losses that are created instantaneously in the photoemission process (Mahan-Nozière-DeDominicis effect[10,11]). The neglect of the intrinsic part is safe for Al, because it accounts for at most 15% of the intensity.[7]

ϕ scans

The maxima in the intensity scans in Figs. 1, 2, and 4 always correspond to electron detection along densely packed rows of atoms in the ⟨011⟩ directions. It has been demonstrated recently by Xu *et al.*,[9] that under these conditions, defocusing effects in the forward scattering of the electrons are expected as a result of multiple-scattering processes. In particular, Xu *et al.* show that the forward-scattering enhancement associated with near-neighbor scattering along the [011] direction ($\theta = 45°$, $\phi = 0°$) from a Cu(001) and Ni(001) surface is completely destroyed by multiple-scattering effects, if the emitter is the 5th atom below the surface in the [011] row. Already, for a chain of three atoms (emitter and two scatterers below the surface) the scattered intensity is reduced in the multiple-scattering case as compared to the situation where only single-scattering events are taken into account.

Although these calculations do not directly apply to Al, we shall make a qualitative comparison of these calculations with our data. If we assume an isotropic mean free path Λ_{tot} of the electrons, about two-thirds of the observed photocurrent originate from a depth Λ_{tot} along the trajectory of the electron detection direction below the surface. For the 1*s* line of Al, with a kinetic energy of 180 eV and a corresponding total mean free path of

≈ 5 Å, this means that approximately two-thirds of the photocurrent along [011] come from the first three layers. (Al is fcc with $a_0 = 4.05$ Å and a nearest-neighbor distance of $a_0/\sqrt{2} = 2.86$ Å.) On the other hand, for the 2*s* line ($E_{kin} = 1136$ eV) two-thirds of the photocurrent originate from the eight first layers below the surface. Using the results by Xu *et al.*[9] for Cu chains, and assuming that defocusing effects destroy the anisotropies of emitters below the fifth layer completely, one would expect a reduction of the overall anisotropy of the 2*s* line of 50%, with respect to that of the 1*s* line. Actually, however, at the same resolution of $\Delta\Omega \leq 3°$, the anisotropies are the same (compare Figs. 1 and 4). One must therefore look for a factor that will offset the effect of the mean free path. The kinetic energy of the 1*s* line is 180 eV and that of the 2*s* line 1136 eV. Since the magnitude of forward scattering increases with increasing kinetic energy, the XPD effect will be enhanced for the 2*s* line relative to that of the 1*s* line, making the overall effect more equal, in agreement with our observation.

We shall now show how the XPD data from the plasmon-loss peaks accompanying the 1*s* and 2*s* lines can be used to arrive at more quantitative conclusions about the defocusing effect. We emphasize, however, that in view of the complexity of the problem, our conclusions must remain vague at this point. Assuming that the creation of plasmons is an independent process, the creation probability for *n* plasmons as a function of the depth *d* of the photoemitter below the surface can be calculated and is given in Fig. 5 for $n = 0$ (main line), 1, and 2.[5] In this estimate the plasmon creation length Λ_{pl} was set equal to the total mean free path Λ_{tot}, a procedure also used by Raether.[5] Since the exact magnitude of the ratio $\Lambda_{pl}/\Lambda_{tot}$ is not known, and since it is of the order of unity [the analysis in Ref. 7(a) gives a value of 1.4 for this ratio], this approximation is not unreasonable. The curves in Fig. 5 show Poisson distributions that peak at 0, 1, and 2 times Λ_{tot} for the creation of zero, one and two bulk plasmons, respectively. The width of these distributions increases with increasing *n*. Figure 5 also indicates

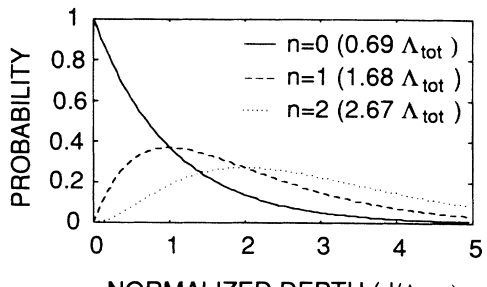

FIG. 5. Detection probability of photoelectrons with $n = 0$, 1, and 2 plasmon losses as a function of the reduced depth d/Λ_{tot} in a homogeneous medium. These distributions show a maximum at $d/\Lambda_{tot} = n$. The numbers in parentheses give the depth from below which 50% of the electrons having experienced *n* plasmon losses originate, therefore representing a median depth of emission. Λ_{pl}, which is the mean free path for the creation of a discrete plasmon loss, is chosen to be equal to Λ_{tot}.

the depth within which 50% of the electrons having experienced $n = 0$, 1, and 2 plasmon losses are produced. This depth therefore represents a median emission depth of the respective electrons. In the no-loss line we obtain a value of 0.69 Λ_{tot}. However, 50% of the electrons contained in the first plasmon-loss line have an origin deeper than $1.68\Lambda_{tot}$. The electrons in the second bulk plasmon originate from an even broader spacial area with more than 50% coming from deeper than $2.67\Lambda_{tot}$ below the surface. With $\Lambda_{tot} = 20$ Å at a kinetic energy of about 1100 eV, the electrons in the first bulk plasmon come from a median depth of ≈ 34 Å below the surface, and those in the second plasmon from ≈ 53 Å below the surface. It is evident from the data in Fig. 2 that between the first and second plasmon production the forward-scattering effect along the [011] direction gets wiped out. This gives us an approximate value of ≈ 45 Å for the length over which this forward-scattering effect exists. This number is much longer than the defocusing length calculated by Xu *et al.* for Cu chains.[9]

This large difference between the calculation by Xu *et al.*[9] and our data needs a comment. The calculations of Xu *et al.*[9] were performed for Cu, whereas our experiments were performed on Al, and it is not evident what kind of changes the calculations produce as a function of atomic number. This point has to be checked. Secondly, one may suggest that it is a very large intrinsic contribution to the plasmon production, that produces the anomalous behavior in the intensities of the XPD patterns. Unfortunately, the available data on this point are very conflicting.

The plasmons accompanying a core line in photoemission can be described[7] as $I_n = b^n/n! + aI_{n-1}$, where *n* numbers the plasmons and *b* and *a* are the intrinsic and extrinsic plasmon creation rate, respectively; the intensity of the zero-loss line I_0 is normalized to unity in this formula. If one assumes that $a = 0.65$, which the data[7] seem to agree upon, for the intrinsic contribution to the first plasmon peak one gets 15, 24, and 38% using $b = 0.1$, 0.2, and 0.4, respectively; for the second plasmon peak the corresponding percentages are 1, 4, and 11%. As far as *b* for Al goes, the analysis of Steiner *et al.*[7(a)] yields 0.1, that of Pardee *et al.*[7(b)] $(b/a) \ll 0.1$, that of Penn[7(c)] 0.2 (this author quotes no number, so it has to be extracted from the text with the corresponding uncertainty) and that of van Attekum and Trooster[7(d)] 0.2. All these authors use very different forms of data analyses, and this may be responsible for the large spread in the results. However, it seems that any reasonable data analysis rules out values for *b* that are larger than 0.2, and that the most likely value is $b = 0.10 \pm 0.05$. Any value below $b = 0.2$ can, however, not explain the large drop in XPD anisotropy seen in Fig. 2, and even an unreasonable high value of $b = 0.4$ could not account for the high anisotropy seen in the first plasmon peak. We are therefore left with the conclusion that calculations of the defocusing length for Al have to be performed along the lines of Xu *et al.*[9] before a final judgement on the data of Fig. 2 can be given.

Plasmon creation does also involve a small change in momentum of the primary electron. The main intensity

of the scattered electrons after the production of one plasmon goes into a cone with a total opening angle of $E_{PL}/E_0 \approx 1°$, where E_0 is the primary energy of the electron, which is taken here as 1000 eV.[5] Thus, even after the production of two plasmons, a total divergence of the primary electron beam of 2° should fall into the acceptance angle of 3° chosen for the experiments involving plasmon creation. Therefore defocusing by plasmon production cannot be the main reason for the drop in relative intensity in the [011] maxima for successive plasmon lines as shown in Figs. 1 and 2.

This is substantiated by another finding. The relative anisotropy measured for the smaller maxima at ±30° from the [011] direction is ≈20%, and it is the same in the main line, the first, the second, and the third plasmon-loss peaks. This confirms that defocusing by plasmon scattering is a weak effect. Defocusing by multiple elastic scattering on the other hand appears to critically depend on the distance and the direction of adjacent scatterers, and it is practically absent in the crystallographic directions leading to these smaller maxima in the diffraction patterns.

Energy scans

It has been found from an analysis of the plasmon-loss peaks that accompany the core lines of Na, Mg, and Al, that the mean free path for plasmon creation Λ_{pl} is, approximately, proportional to the total mean free path[7] with $\Lambda_{pl}/\Lambda_{tot}=\frac{3}{2}$, while theoretical considerations give a value of about 2 for this number.[5,6] However, these experiments used kinetic energies $E_{kin} \geq 400$ eV. Here we present data with the Al 1*s* line, having a kinetic energy of only 180 eV for the zero-loss line. From Fig. 3 it is obvious that at this kinetic energy the value $\Lambda_{pl}/\Lambda_{tot}$ is larger than that for the 2*s* line ($E_{kin}=1136$ eV) because the 1*s* line shows less discrete loss structure than the 2*s* line. The reason for this finding may be associated with the small total escape depth ($\Lambda_{tot} \approx 5$ Å) for electrons with $E_{kin}=180$ eV in Al. At these small energies the probability for the creation of losses by electron-hole–pair production and electron-ion scattering increases as compared to the situation at higher kinetic energy, giving rise to additional continuous-loss intensity. Also, the ratio of surface-to-volume plasmon-loss production increases, as is evident from the data.

A comparison of the two 2*s* spectra taken at an intensity maximum of the no-loss azimuthal scan ([011] direction) and at a local minimum 45° away from the [011] direction (see Fig. 3) shows that the apparent bulk plasmon creation rate is smaller in the direction of maximum no-loss intensity than in that of minimum intensity. This is only another way of viewing the data in Figs. 1 and 2. To be more quantitative: in the direction of maximum no-loss intensity ([011] direction) we have a plasmon production rate of $a_{max}=I_n/I_{n-1} \approx 0.4$, and in the direction of minimum intensity $a_{min}=I_n/I_{n-1} \approx 0.6$. This latter number is close to the one obtained from a polycrystalline sample, namely $a_{poly}=\frac{2}{3}$ (I_n is the integrated intensity in the *n*th plasmon-loss peak accompanying the main line with intensity I_0).[7] In terms of the mean free paths one has $a=\Lambda_{tot}/\Lambda_{pl}$.

It is in this respect interesting to realize that the two spectra for Al 2*s* obtained at equal conditions, except different azimuthal settings ϕ (Fig. 3), end up with almost the same height of the background far beyond the main line ($E_{kin} < 1050$ eV). A precise measurement ($\Delta\Omega < 3°$) of the total background signal in the energy window between 1040 and 1047 eV reveals a small but measurable anisotropy of 6.5% in a azimuthal scan at $\theta=45°$. In this background scan we find minima along the ⟨011⟩ directions.

These latter findings confirm the observation made by Egelhoff[12] on a Cu(001) surface, indicating that large XPD effects are limited to a relatively narrow spectral range around a photoemission line, outside which the background shows much less anisotropy. Apparently, XPD is a spacially, rather short-range process that focuses main-line intensities into directions of high atomic densities (like the [011] direction), but leaves the longer-range inelastic tails less affected.

Comparison to theory

The measured XPD curves are compared with the results of single-scattering calculations, for which a cubic cluster of 3×3×3 unit cells was used (see Fig. 4). These calculations reproduce the triangle-shaped main signals that arise from the [011] scattering directions quite well. The comparison of the results for the 2*s* and 1*s* line also indicates the effects of reducing the kinetic energy from 1136 to 180 eV. The reduced kinetic energy results in a larger electron wave length, a smaller mean free path, and in a less pronounced forward-scattering effect for the scattered electrons. All these effects will tend to suppress fine structure in the diffraction patterns and also reduce the sharpness of the main signals, which is actually observed in the data and also reproduced in the calculations.

In the theoretical simulations, we have made the observation that the agreement between theory and experiment gets worse if the cluster size is increased. The calculated diffraction patterns show structures that are not observed in the experimental patterns. A similar problem had been encountered in the interpretation of high-resolution XPD data from Ni(001).[13] In a corresponding Ni $2p_{3/2}$ azimuthal scan at $\theta=45°$ a 3×3×3 unit-cell cluster calculation shows rather good agreement with experiment. The calculations employing a 6×6×6 cluster, however, led to diffraction patterns which, by comparing them with the measured ones, can be interpreted as overemphasizing the first-order, Bragg-related peaks relative to the zero-order forward-scattering peaks. Of course this division is quite artificial, but it allows to discriminate those peaks in the XPD patterns that can be viewed as originating from forward scattering along rows of atoms, and which will not move when the kinetic energy is varied, from those that are a result of more complicated scattering, such as from Bragg planes.

In order to come to an understanding of the defocusing effects in Al we are presently performing multiple-scattering calculations. First results suggest that the conclusions obtained by Xu *et al.*[9] for Cu chains cannot be

generally applied to different crystals and photoelectron energies, at least not in a quantitative way.

Comparison with other electron-scattering data

We shall now try to compare the present XPD results on Al with similar investigations involving Kikuchi electrons from Al(001) (Ref. 14) and Ni(001) (Ref. 15) crystals. Kikuchi electrons originate from an inelastic scattering of a primary beam of monoenergetic electrons in a crystal. These Kikuchi electrons are Bragg reflected from low-index crystal planes and thereby give rise to the well-known lines seen in electron-scattering experiments with primary energies E_p of more than 500 eV. For the quasielastic peak at a primary energy of 1000 eV Mosser *et al.*[14] find a polar intensity distribution in a (001) plane quite similar to the one seen in the present XPD experiment (not shown here), with a pronounced maximum at $\theta=45°$, i.e., along the [011] direction. For an energy loss of $\Delta E=15$ eV (first bulk plasmon), this maximum appears to be slightly reduced in intensity relative to the background. This is similar to the trend seen in the present XPD data. The data of Mosser *et al.*[14] also show that at an energy loss of $\Delta E=100$ eV the anisotropy in the Kikuchi-electron intensities has practically disappeared, again in agreement with the present XPD data. It looks as if photoelectrons and Kikuchi electrons of the same kinetic energy show very similar scattering patterns in the same crystal. Therefore, a theoretical approach that explains the Kikuchi-electron intensities and which is in essence a Bragg-type calculation[14] must also be able to explain XPD patterns. This does not invalidate the cluster-type calculations presented here that are very successful in analyzing XPD data; the cluster calculations are indeed less time consuming and therefore more practical than the Bragg scattering theories.

Auger electrons can, apart from the excitation process, be viewed very much like photoelectrons. It has been found that Auger electrons and Kikuchi electrons show again quite similar diffraction patterns,[15,16] and also that a cluster theory yields a very satisfactory description of both types of data.[16] It therefore seems that photoelectrons, Auger electrons, and Kikuchi electrons behave in a similar way in a crystal, as far as their scattering and diffraction is concerned. This implies that the theoretical models used to describe the diffraction patterns should be identical. However, while photoelectron and Auger electron diffraction are usually described by cluster calculations, Kikuchi electrons are analyzed within a Bragg scattering picture. This is understandable from a historical point of view, it is, however, not necessitated from physical considerations.[17,18]

CONCLUSIONS

Photoelectron diffraction from the 2*s* and 1*s* core lines of Al(001) yields well-developed diffraction patterns that can be described by a single-scattering theory employing a small $3\times3\times3$ unit-cell cluster. Setting the energy window on the plasmon-loss peaks accompanying the 2*s* core level allows us to estimate the defocusing length for the scattering along [011] rows of atoms. If currently available data on the intrinsic plasmon creation rate in Al are considered, the major part of the plasmon-loss signals are due to extrinsic plasmon creation, i.e., the plasmon number is a measure of the depth at which the original photoelectron was created. The rate at which the forward-scattering maxima along $\langle 011 \rangle$ directions are suppressed with increasing n then indicates a defocusing length in Al of the order of 45 Å. This is much longer than that predicted by a recent multiple-scattering analysis of defocusing effects along linear Cu chains.[9,19] A more detailed theoretical analysis of such effects is thus necessary, including the dependence on atomic number, interatomic distance within the chain, and the kinetic energy of the photoelectrons.

Apart from the defocusing effects observed along [011] rows, the plasmon-loss diffraction patterns show the same structures as the no-loss data, indicating similar scattering and diffraction of these inelastic features. This is a further argument for that photoelectrons, Auger electrons, and Kikuchi electrons all should show similar diffraction patterns, which should make them tractable by the same sort of theory.

ACKNOWLEDGMENTS

One of the authors (S.H.) thanks the Institut de Physique de l'Université de Fribourg for its hospitality and a most stimulating and friendly research atmosphere. This work has been supported by the Schweizerischer Nationalfonds.

*Permanent address: Fachbereich Physik, Universität des Saarlandes, D-6600 Saarbrücken, FRG.

[1]C. S. Fadley, Prog. Surf. Sci. **16**, 275 (1984); C. S. Fadley, Phys. Scr. T **17**, 39 (1987).

[2]M. Sagurton, E. L. Bullock, and C. S. Fadley, Surf. Sci. **182**, 287 (1987).

[3]H. J. Levinson, F. Greuter, and E. W. Plummer, Phys. Rev. B **27**, 727 (1983).

[4]H. Höchst, P. Steiner, and S. Hüfner, Z. Phys. B **30**, 145 (1987).

[5]H. Raether, *Excitation of Plasmons and Interband Transitions by Electrons*, Vol. 88 of *Springer Tracts in Modern Physics*, edited by G. Höhler and E. A. Niekisch (Springer, Heidelberg, 1980).

[6]D. R. Penn, J. Electron Spectrosc. Relat. Phenom. **9**, 29 (1976).

[7](a) P. Steiner, H. Höchst, and S. Hüfner, Z. Phys. B **30**, 129 (1987); (b) W. J. Pardee, G. D. Mahan, D. E. Eastman, R. A. Pollak, L. Ley, F. R. McFeely, S. P. Kowalczyk, and D. A. Shirley, Phys. Rev. B **11**, 3614 (1975); (c) D. R. Penn, Phys. Rev. Lett. **38**, 1429 (1977); (d) P. M. Th. M. van Attekum, and J. M. Trooster, Phys. Rev. B **18**, 3872 (1978).

[8]S. Y. Tong, H. C. Poon, and D. R. Snider, Phys. Rev. B **32**, 2096 (1985).

[9]M. L. Xu, J. J. Barton, and M. A. Van Hove, Phys. Rev. B **39**, 8275 (1989).

[10]G. D. Mahan, Phys. Rev. **163**, 612 (1967).

[11]P. Nozière and C. T. De Dominicis, Phys. Rev. **178**, 1097

(1969).
[12]W. F. Egelhoff, Jr. Phys. Rev. B **30**, 1052 (1984).
[13]J. Osterwalder, A. Stuck, D. J. Friedman, A. Kaduwela, C. S. Fadley, J. Mustre de Leon, and J. J. Rehr, Phys. Scr. (to be published).
[14]A. Mosser, Ch. Burggraf, S. Goldsztaub, and Y. H. Ohtsuki, Surf. Sci. **54**, 580 (1976).
[15]H. Hilferink, E. Lang, and K. Heinz, Surf. Sci. **93**, 398 (1980).
[16]H. Cronacher, K. Heinz, K. Müller, M. L. Xu, and M. A Van Hove, Surf. Sci. **209**, 387 (1989).
[17]W. Schaich, Phys. Rev. B **8**, 4078 (1973).
[18]R. Trehan, J. Osterwalder, and C. S. Fadley, J. Electron. Spectrosc. Relat. Phenom. **42**, 187 (1987).
[19]The estimate of the defocusing length assumes that the process of plasmon creation does not destroy the phase of the photoelectron wave. In analogy to the neutron spin-flip experiment described in *The Feynman Lectures in Physics* (Addison-Wesley, Reading, MA, 1965), Vol. III, pp. 3–8, one may expect some loss of coherency due to the localized character of plasmon creation. A gedanken experiment may be designed that permits one to locate the site of the plasmon creation to some degree, therefore rendering all scattering amplitudes obsolete that do not include this particular site. Only scattering events after the plasmon creation would then exhibit coherent scattering and interference. Considering such effects, our estimate of 45 Å for the defocusing length in Al at $E_{\text{kin}} = 1136$ eV is an upper limit for that quantity.